

# Characterization of a Cyclosporine Solid Dispersion For Inhalation

Submitted: March 13, 2007; Accepted: May 14, 2007; Published: June 15, 2007

Gerrit S. Zijlstra,<sup>1</sup> Michiel Rijkeboer,<sup>1</sup> Dirk Jan van Drooge,<sup>1</sup> Marc Sutter,<sup>3</sup> Wim Jiskoot,<sup>2,3</sup> Marco van de Weert,<sup>4</sup> Wouter L.J. Hinrichs,<sup>1</sup> and Henderik W. Frijlink<sup>1</sup>

<sup>1</sup>Department of Pharmaceutical Technology and Biopharmacy, University of Groningen, Groningen, The Netherlands

<sup>2</sup>Department of Pharmaceutics, Utrecht Institute for Pharmaceutical Sciences (UIPS), Utrecht, The Netherlands

<sup>3</sup>Division of Drug Delivery Technology, Leiden/ Amsterdam Center for Drug Research (LACDR), Leiden, The Netherlands

<sup>4</sup> Department of Pharmaceutics and Analytical Chemistry, Faculty of Pharmaceutical Sciences, University of Copenhagen, Copenhagen, Denmark

## ABSTRACT

For lung transplant patients, a respirable, inulin-based solid dispersion containing cyclosporine A (CsA) has been developed. The solid dispersions were prepared by spray freeze-drying. The solid dispersion was characterized by water vapor uptake, specific surface area analysis, and particle size analysis. Furthermore, the mode of inclusion of CsA in the dispersion was investigated with Fourier transform infrared spectroscopy. Finally, the dissolution behavior was determined and the aerosol that was formed by the powder was characterized. The powder had large specific surface areas ( $\sim 160 \text{ m}^2$ ). The water vapor uptake was dependant linearly on the drug load. The type of solid dispersion was a combination of a solid solution and solid suspension. At a 10% drug load, 55% of the CsA in the powder was in the form of a solid solution and 45% as solid suspension. At 50% drug load, the powder contained 90% of CsA as solid suspension. The powder showed excellent dispersion characteristics as shown by the high emitted fraction (95%), respirable fraction (75%), and fine-particle fraction (50%). The solid dispersions consisted of relatively large ( $x_{50} \approx 7 \mu\text{m}$ ), but low-density particles ( $\rho \approx 0.2 \text{ g/cm}^3$ ). The solid dispersions dissolved faster than the physical mixture, and inulin dissolved faster than CsA. The spray freeze-drying with inulin increased the specific surface area and wettability of CsA. In conclusion, the developed powder seems suitable for inhalation in the local treatment of lung transplant patients.

**KEYWORDS:** DPI, Cyclosporine A, solid dispersion, FTIR, aerosol, large porous particles

## INTRODUCTION

To improve immunosuppressive therapy in lung transplant patients, studies with inhalation of cyclosporine A

(CsA, Figure 1) have been conducted.<sup>1,2</sup> The overall survival of lung transplant patients increased dramatically when aerosolized CsA was administered on top of base therapy.<sup>3</sup> The formulation for inhalation used in the published study was a solution of CsA in propylene glycol. A disadvantage of this approach was that nebulization of propylene glycol caused extreme irritation in the airways, which was reduced by the use of aerosolized local anesthetics. Despite the use of local anesthesia, a substantial number of patients ( $\pm 10\%$ ) could not complete the study because of extreme irritation.<sup>4</sup> Apparently there is a need for a less-irritating formulation for inhalation. A second disadvantage of nebulization of CsA dissolved in propylene glycol is the low deposition efficiency, which has been reported to be 5.4% to 11.2% of the metered dose,<sup>4</sup> which is consistent with other studies on nebulization.<sup>5-7</sup> To obtain a significant improvement in pulmonary function in lung transplant patients with chronic rejection requires a deposition of at least 5 mg CsA in the lower airways (peripheral part of the lung),<sup>1</sup> which can only be achieved by high metered doses. This further underlines the need for more effective formulations for inhalation. A third problem is the lipophilicity of CsA (aqueous solubility of 3.69 mg/L at 37°C,  $\log P = 3.0$ ),<sup>8,9</sup> which limits the choice of solvents for nebulization.

We proposed that a dry powder formulation consisting of a solid dispersion could overcome these problems. Firstly, with dry powder inhalation the use of local anesthesia and irritating solvents can be avoided. Secondly, the higher deposition efficiency of dry powder inhalation compared with nebulization reduces the need for high metered doses.<sup>10</sup> Finally, solid dispersions are known for their dissolution rate-enhancing properties of poorly soluble drugs, such as CsA.<sup>11-13</sup> The dissolution rate of poorly soluble drugs from inulin-based solid dispersions has been shown to increase when compared with the pure hydrophobic drug.<sup>14</sup>

A powder for local administration in lung transplant patients should meet two requirements. First, the drug substance should dissolve within a reasonable time span, since removal of particles by mucociliary clearance occurs within a couple

---

**Corresponding Author:** Gerrit S. Zijlstra, Department of Pharmaceutical Technology and Biopharmacy, University of Groningen, The Netherlands, Antonius Deusinglaan 1, 9713 AV Groningen, The Netherlands. Tel: +31 50 363 3172; Fax: +31 50 363 2500; E-mail: G.S.Zijlstra@rug.nl

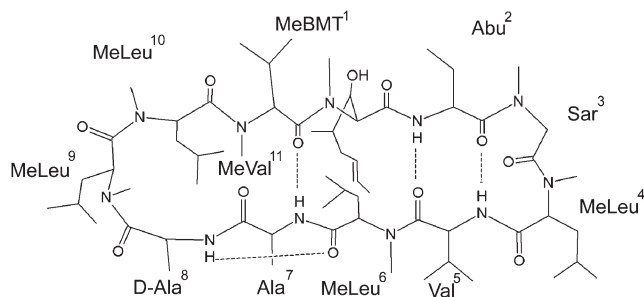


**Figure 1.** Molecular structure of Cyclosporine A.

of hours.<sup>15,16</sup> Second, the powder should have an aerodynamic size range that is suitable for inhalation (1 to 5  $\mu\text{m}$ ).<sup>17,18</sup> Regarding the first requirement, benefit may be gained with a rapidly dissolving dry powder formulation. The second requirement can be met by using spray freeze-drying as production method.<sup>19-21</sup>

The purpose of this study was to develop a powder for inhalation as an alternative for nebulized CsA. We investigated the feasibility of an inulin-based solid dispersion with CsA. CsA in the solid dispersion can be distributed as separate molecules, defined as a solid solution, or as multimolecular clusters of CsA, defined as a solid suspension or as a combination of both.<sup>22</sup> The type of solid dispersion of CsA in inulin, eg, solid solution, solid suspension or a combination of both, was investigated with Fourier transform infrared (FTIR) spectroscopy. Furthermore, other physical characteristics relevant for the performance as powder for inhalation were investigated.

## MATERIALS AND METHODS

### Materials

CsA was obtained from LC Labs (Woburn, MA). Inulin, with an average degree of polymerization of 23 was a generous gift from Sensus (Roosendaal, The Netherlands). *Tert*-butyl alcohol (TBA), methanol, acetonitrile, sodium dodecyl sulfate (SDS), KBr, and anthrone reagent were of the highest available grade of purity (KBr was spectroscopy grade) and purchased from commercial suppliers. The water used in the experiments was demineralized.

### Methods

#### Sample preparation

The CsA solid dispersions were produced as described previously.<sup>20</sup> Briefly, CsA was dissolved in TBA and inulin in water. Next, the solutions were mixed at a TBA/water ratio of 40/60 vol/vol. The concentrations of CsA in TBA and inulin in water were chosen such that the combined mass of CsA and inulin in the solution was constant (5% wt/vol) while the drug load varied. Immediately after mixing, the

resulting TBA/water solution was sprayed onto liquid nitrogen with a heated 2-fluid nozzle (orifice 0.5 mm, atomizing airflow 500 L/h, liquid flow 6 mL/min). The solutions did not show any phase separation as indicated by clearness of the solution during processing. On completion of spraying, the liquid nitrogen was evaporated and the frozen droplets were freeze-dried in a Christ model Alpha 2-4 lyophilizer (Salm and Kipp, Breukelen, The Netherlands). The shelf temperature of the lyophilizer was maintained at  $-35^{\circ}\text{C}$  with a pressure of 0.220 mbar for 24 hours. The temperature was then gradually increased to  $20^{\circ}\text{C}$ , while the pressure was decreased to 0.050 mbar. These conditions were maintained for another 24 hours. During the whole freeze-drying process the condenser temperature remained at  $-55^{\circ}\text{C}$ . After freeze-drying, the samples were stored over silica gel in a vacuum desiccator until analysis.

### Chemical analysis

The drug content and concentration during dissolution was determined by a high-performance liquid chromatography (HPLC) method,<sup>23</sup> which was slightly modified for our purpose. In short, undiluted samples (100  $\mu\text{L}$ ) were injected using a Gilson 234 auto injector (Gilson, Middleton, WI) on a reversed phase C8 column (5- $\mu\text{m}$  Hypersil BDS 250  $\times$  4.6 mm, Thermo Hypersil Ltd, Runcorn, UK) equipped with a thermostat (Jones Chromatography model 7990, Hogoed, UK) at  $70^{\circ}\text{C}$ . A flow rate of 0.9 mL/min of the mobile phase (85/15 acetonitrile/water) was maintained with a Waters model 510 pump (Waters, Milford, MA). Detection of CsA was performed with a Waters 490 programmable wavelength detector 212 nm. These settings resulted in an elution time for CsA of  $\sim 6$  minutes. The obtained data were analyzed with KromaSystem 2000 software version 1.83 (Winooski, VT). All measurements were performed in triplicate. Drug content was within  $\pm 2.5\%$  of the theoretical drug content and dissolution of CsA was  $100\% \pm 2.5\%$  of the metered dose for dissolution.

The concentration of inulin during dissolution was determined by the anthrone assay.<sup>24</sup> Samples of 0.25 mL were diluted with water to 1.00 mL. Subsequently, 2.00 mL of a freshly prepared 0.1% wt/vol anthrone reagent in concentrated sulfuric acid was added and immediately vortexed. The mixture heated up because of the exothermic character of the reaction enthalpy of mixing. After cooling to room temperature, samples (200  $\mu\text{L}$ ) were pipetted into a 96-well plate and analyzed spectrophotometrically at 630 nm in a plate reader (Benchmark plate reader, BioRad, Hercules, CA). A freshly prepared calibration curve of inulin (0 to 0.100 mg/mL, 11 points) was measured for each determination. All measurements were performed in triplicate.

### Physical characterization of samples

Specific surface areas of the formulations were measured using the Brunauer, Emmett, and Teller (BET) method with a Tristar 3000 model (Micromeritics, Norcross, GA). The measured samples were placed into test tubes and purged for at least 3 hours with helium at 30°C to evaporate residual moisture. Subsequently, a 9-point isotherm was recorded at a sample temperature of -196°C (liquid nitrogen).

The vapor sorption behavior of the solid dispersions at 25°C was determined by dynamic vapor sorption (DVS 1000, Surface Measurement Systems Ltd, London, UK). About 10 mg of material was weighed in the sample cup and exposed to 0% relative humidity (RH) until equilibrium ( $dm/dt < 0.0005\%/min$ ) was reached. The RH was subsequently increased to 30%. An RH of 30% was chosen because inulin remains in the glassy state upon exposure to 30% RH at 25°C.<sup>9,25</sup>

Changes in the secondary structure of CsA caused by spray freeze-drying and incorporation in inulin were studied with FTIR spectroscopy. Powder samples were prepared by mixing approximately 2 to 3 mg of the different CsA formulations with approximately 300 mg KBr. These mixtures were compacted into a 13-mm disc at 37 MPa pressure with a hydraulic press. The liquid sample was prepared by dissolving CsA in a mixture of methanol and acetonitrile. Water was gently added to obtain a concentration of 100 mg/mL and volume percentages of 32% methanol (MeOH), 32% acetonitrile (ACN), and 36% H<sub>2</sub>O. Spectra of dry powders were recorded on a Bio-Rad FTS6000 FTIR spectrometer with Win-IR Pro software (Cambridge, MA). 256 Scans were co-added at a resolution of 2 cm<sup>-1</sup> and scan speed of 0.16 cm/s (5-kHz laser modulation). Spectra of CsA in the cosolvent solution were collected by averaging 1024 scans. All absorbance spectra were corrected for water vapor and if necessary for the cosolvent solution.<sup>26</sup> The measured spectra were smoothed with a 13-point Savitzky-Golay function<sup>27</sup> and second derivative spectra were calculated. The derivative spectra were also smoothed with a 13-point Savitzky-Golay function and inverted.

To establish similarity of the unresolved amide I bands, the specific area overlap was determined.<sup>28,29</sup> The spectra were truncated to contain only the amide I band. Next, the amide I band was baseline-corrected, area-normalized to unity, and exported to a spreadsheet program. The area overlap of 2 spectra, with the amide I band of CsA in the cosolvent solution as reference, was calculated by creation of a new spectrum consisting of the lowest absorption value of the 2 spectra at each data point. The area under this new spectrum corresponds to the percentage area overlap.

### Aerosol characterization

Particle size distributions of the spray freeze-dried samples were measured with a Helos Compact model KA laser diffraction apparatus (100-mm lens, Fraunhofer theory, Clausthal-Zellerfeld, Germany) equipped with an RODOS dry powder dispersing system (Sympatec GmbH, Clausthal-Zellerfeld, Germany) at a pressure difference of 0.5 bar. All measurements were performed in triplicate.

Because the particle size distributions were found to be log-normal, the geometric standard deviation (GSD) was calculated from laser diffraction data as follows<sup>30</sup>:

$$GSD = \sqrt{\frac{x_{84}}{x_{16}}} \quad (1)$$

where  $x_{84}$  and  $x_{16}$  represent the 84% and 16% cumulative undersize diameter, respectively. The aerodynamic diameter, as measured with cascade impactor analysis, depends on the equivalent particle diameter, shape factor, and density<sup>30</sup>:

$$d_{ae} = d_e \sqrt{\frac{\rho_p}{\rho_0 \chi}} \quad (2)$$

where  $d_{ae}$  is the aerodynamic diameter,  $d_e$  the equivalent laser diffraction diameter,  $\rho_p$  the density of the particles (g/cm<sup>3</sup>),  $\rho_0$  the unit density (1 g/cm<sup>3</sup>), and  $\chi$  the dynamic shape factor (1 for spherical particles).

For cascade impactor analysis a multistage liquid impinger (MSLI, Erweka, Heusenstamm, Germany) was used with a test inhaler<sup>31</sup> attached to the induction port. A solenoid valve was used in combination with a timer to control the flow (60 L/min) through the inhaler and the cascade impactor for a duration of 3 seconds. The stages of the cascade impactor were filled with 20 mL of 85/15 vol/vol acetonitrile/water for extraction of CsA from the deposited powder. A total amount of 50 mg was delivered in 10 separate doses. The deposition of the drug on the different stages was measured by HPLC as described above. The deposition was subsequently calculated as the percentage of the metered dose. The emitted fraction was defined as the metered dose minus inhaler retention, the respirable fraction was calculated by the sum of deposition on the second, third, fourth, and filter stage and the fine particle fraction (FPF) was calculated by the sum of deposition on the third, fourth, and filter stage. The emitted fraction, respirable fraction, and FPF are expressed as a percentage of the metered dose. Cascade impactor analysis was performed on only the solid dispersions with 30% and 50% wt/wt drug loads. All experiments were performed in triplicate.

### Dissolution rate

Dissolution experiments were performed using an USP dissolution apparatus I (Rowa Techniek B.V., Leiderdorp, The Netherlands) at 37°C in 1000 mL water containing 0.25%



wt/vol SDS with constant stirring of 100 rpm. Before the dissolution study, a series of solubility tests were conducted with SDS concentrations up to 1% wt/vol to investigate at which SDS concentration sink conditions (maximal concentration =  $0.20 \times C_{\text{saturated}}$ ) were met. At the maximal CsA concentration (30 mg/L) it was found that sink conditions were met at 0.25% SDS (data not shown). The formulations were weighed into the baskets of the dissolution apparatus. For the formulations containing 10%, 20%, 30%, and 50% wt/wt CsA, amounts of, respectively, 300, 150, 100, and 60 mg of powder were weighed to keep the total amount of CsA in the dissolution vessel constant at 30 mg. A physical mixture of 30 mg of spray freeze-dried CsA and 70 mg of spray freeze-dried inulin was used as a reference. Samples were analyzed with HPLC and anthrone assay for determination of the CsA and inulin concentration, respectively. All experiments were performed in triplicate.

## RESULTS AND DISCUSSION

### Physical characterization

The specific surface areas and moisture uptake of the produced solid dispersions are shown in Table 1. Spray freeze-drying generally results in powders with large specific surface areas and the powders in this study are no exception.<sup>20,32,33</sup> The large specific surface area is related to the spray freeze-drying process because with spray freeze-drying the aerosol is rapidly frozen, which causes the formation of a large number of small solvent crystals. Around these small solvent crystals the freeze concentrated fraction is distributed. Solvent removal by freeze-drying thus results in a large specific surface area. The produced batches did not differ substantially in specific surface area, with pure spray freeze-dried CsA as an exception (Table 1). The lower specific surface area of pure spray freeze-dried CsA may be caused by the absence of sugar, which might influence the freezing behavior.

Possible degradation of CsA during spray freeze-drying has not been investigated. However, we have no reason to assume

**Table 1.** Specific Surface Areas and Water Vapor Uptake (at 30% RH and 25°C) of the Spray Freeze-Dried Powders

Batch	Specific Surface Area, Moisture Uptake,	
	m <sup>2</sup> /g	% wt/wt
10% wt/wt CsA	152	6.08
20% wt/wt CsA	185	5.44
30% wt/wt CsA	185	4.84
50% wt/wt CsA	145	3.97
Pure spray freeze-dried CsA	40	1.03

CsA indicates cyclosporine A.

that degradation of CsA did occur during spray freeze-drying for various reasons. First of all, results from drug content analysis and dissolution were all within  $\pm 2.5\%$  of the theoretical drug content and metered dose, respectively, which suggests a complete mass balance for CsA. Second, FTIR did not reveal possible degradation by fingerprint inspection. Furthermore, CsA appears to be a stable compound since it has been processed in several ways without noting degradation in various studies.<sup>34-36</sup> Finally, a chemically less stable compound than CsA,  $\Delta^9$ -tetrahydrocannabinol, has successfully been spray freeze-dried from a TBA/water solution without noticeable degradation,<sup>20</sup> thus showing that spray freeze-drying is a reliable production technique that minimally distorts the formulated compounds.

The produced powders were susceptible to water vapor uptake (Table 1), which was linearly dependent on the drug ratio ( $[\text{moisture content}] = -0.057 \cdot [\text{drug ratio}] + 0.067$ ;  $R^2 = 0.995$ ). Drug ratio was defined as (drug mass)/(drug mass + mass of excipient) without the addition of water vapor. This shows that the solid dispersion behaves like a physical mixture, which indicates that the 2 components remain in the same physical state, irrespective of the drug load. Furthermore, it shows that CsA does not influence the hydrophilicity of inulin and vice-versa, ie, CsA and inulin each absorb a fixed amount of water vapor, irrespective of the drug load.

The linear dependency of moisture uptake versus drug load for inulin-based solid dispersions has been shown before.<sup>22</sup> In that study, van Drooge et al<sup>22</sup> showed that the water vapor sorption of inulin-based solid dispersions was independent of the type of solid dispersion, defined as a fully amorphous solid solution, fully amorphous solid suspension, or a combination of both.<sup>22</sup> The type of solid dispersion is therefore not discernable with only water vapor sorption measurements.

In general, the physical state of solid dispersions can be determined by differential scanning calorimetry (DSC). However, DSC measurements of CsA and inulin result in substantial overlap of thermal events of both components, which makes it difficult to draw unambiguous conclusions about the physical state of the solid dispersion. Fortunately, the secondary structure of CsA, which can be measured with FTIR, has been reported to depend on the physical state.<sup>37,38</sup> Furthermore, FTIR might give information about the type of solid dispersion, based on the secondary structure of CsA.

CsA has 4 amide groups, which, according to Stevenson et al,<sup>37</sup> in a *hydrophilic* environment result in *intermolecularly* oriented hydrogen bonds. In contrast, a *lipophilic* environment results in *intramolecularly* oriented hydrogen bonds. In the case of a solid solution, the amide groups are hypothesized to be *intermolecularly* oriented because of hydrogen bond interaction with inulin. Conversely, in a solid suspension,

the amide groups are predominantly intramolecularly oriented because of the lipophilic CsA clusters. A combination of a solid solution and suspension should thus result in both inter- and intramolecularly orientated amide groups, in a ratio that would be dependent on the drug load.

### Secondary structure of CsA

First, 2 control samples, CsA in the crystalline state and dissolved in a cosolution of methanol/acetonitrile/water, were measured to show the effect of full intra- and intermolecular orientation of the amide groups, respectively. Bands were assigned according to previously published data.<sup>37</sup>

In the crystalline state (Figure 2A), the 4 amide groups in the CsA molecule (Figure 1) are assumed to be intramolecularly oriented to allow intramolecular hydrogen bonds.<sup>37</sup> In contrast, when CsA was dissolved in the cosolvent solution (Figure 2B), the amide groups are assumed to be directed outward to allow hydrogen bonding with the solvent.<sup>37</sup> Specifically, dissolution of CsA in the cosolvent solution compared with CsA in the crystalline state results in a  $\beta$ -sheet

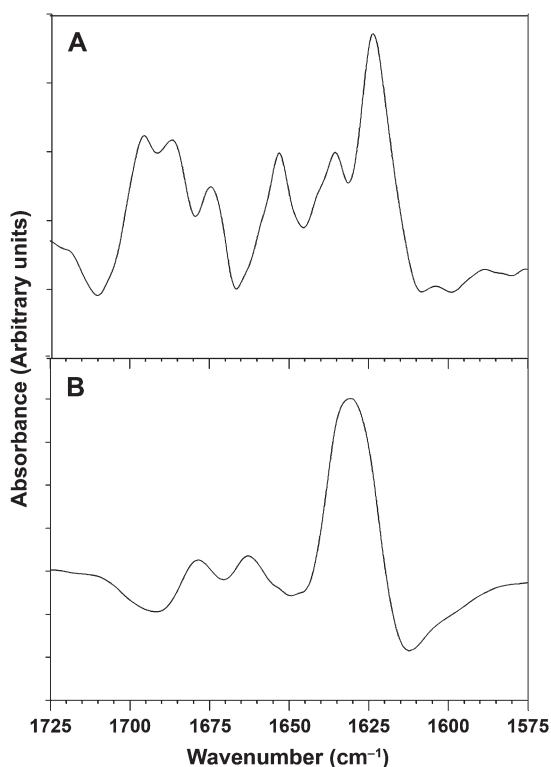


**Figure 2.** Second derivative FTIR spectra of the CsA crystalline control (A) and a solution of 10% (wt/vol) of CsA in 32% MeOH/32% ACN/36% (wt/vol) H<sub>2</sub>O (B). Peak wavenumbers in the crystalline control (A): 1624 (antiparallel  $\beta$ -sheet), 1636 (loose  $\beta$ -sheet), 1653 ( $\gamma$ -loop), 1674 (type-II  $\beta$ -turn), 1688 (MeBMT-turn), and 1695 cm<sup>-1</sup> (aggregate  $\beta$ -sheet); peak wavenumbers in the cosolvent solution (B): 1630 ( $\beta$ -sheet), 1663 ( $\gamma$ -turn), and 1678 cm<sup>-1</sup> (type-II  $\beta$ -turn). See also Table 2.

band at higher wave numbers, which is indicative of a looser  $\beta$ -sheet structure (Table 2). Furthermore, the  $\gamma$ -loop changed into a  $\gamma$ -turn upon dissolution in the cosolvent solution, which is associated with a change in orientation of the bond between MeLeu<sup>9</sup> and MeLeu<sup>10</sup> from cis to trans.<sup>37</sup> This change in orientation is caused by the hydrogen bond between D-Ala<sup>8</sup>NH and MeLeu<sup>6</sup>C=O, which bifurcates to include the D-Ala<sup>8</sup>C=O and solvent. The sharing of the amide proton between 2 carbonyls and solvent twists the backbone conformation at D-Ala,<sup>8</sup> by which the orientation of the MeLeu<sup>10</sup> side chain changes. Finally, if the MeBMT<sup>1</sup> side chain (see Figure 1) is in proximity to the backbone, as is the case in the crystalline state, then the  $\beta$ -OH is able to bond with MeBMT<sup>1</sup>C=O, resulting in an MeBMT-turn.<sup>37</sup> Clearly, the MeBMT-turn is not present upon dissolution of CsA in the cosolvent solution, which indicates that the MeBMT<sup>1</sup> side chain is directed outward to interact with the solvent.

If the type of solid dispersion of CsA and inulin would be a solid solution, then the amide groups of CsA would be intermolecularly oriented. Therefore, in a solid solution, the FTIR spectrum of CsA should have the  $\beta$ -sheet band at high wavenumbers ( $\sim$ 1630 cm<sup>-1</sup>), contain a  $\gamma$ -turn band ( $\sim$ 1663 cm<sup>-1</sup>), and the MeBMT-turn band ( $\sim$ 1685 cm<sup>-1</sup>) should be absent. In contrast, if the type of solid dispersion would be a solid suspension, then the amide groups would be intramolecularly oriented, resulting in an FTIR spectrum with a  $\beta$ -sheet band at low wavenumbers ( $\sim$ 1624 cm<sup>-1</sup>), a  $\gamma$ -loop band ( $\sim$ 1653 cm<sup>-1</sup>) and the MeBMT-turn band at  $\sim$ 1685 cm<sup>-1</sup>. A combination of a solid solution and a solid suspension should contain variable amounts of each structural feature, depending on the drug load.

CsA in the inulin solid dispersions (Figures 3A to 3D) apparently has few outward-oriented amide groups as all solid dispersions, as well as pure spray freeze-dried CsA (Figure 3E), contain a  $\beta$ -sheet,  $\gamma$ -loop, and MeBMT-turn. The peak position of the  $\beta$ -sheet band of the solid dispersions and pure spray freeze-dried CsA is in between of the peak positions seen in the crystalline state and in the cosolvent solution (Table 2). Furthermore, the presence of the  $\gamma$ -loop and the absence of the  $\gamma$ -turn in the secondary structure indicate that CsA adopts a cis orientation between MeLeu<sup>9</sup> and MeLeu.<sup>10</sup> Finally, the presence of the MeBMT-turn indicates that the MeBMT<sup>1</sup> side chain is in the proximity of the backbone. At higher drug loads, the relative intensity of the MeBMT-turn seems to increase.

Based on the data obtained by measurement of the secondary structure of CsA in the solid dispersion, the type of solid dispersion can best be described as a combination of a solid solution and suspension. First, the peak position of the  $\beta$ -sheet band of the solid dispersions and pure spray freeze-dried CsA indicates that the type of solid dispersion is a

**Table 2.** Peak Positions of Structural Elements in the Secondary Structure of Cyclosporine A

<i>Data from Stevenson et al.<sup>37</sup></i>							
Sample	$\beta$ -sheets* <sup>1</sup>		$\gamma$ -loop	$\gamma$ -turn	Type-II $\beta$ -turn	MeBMT turn	Aggregate $\beta$ -sheet
Cosolvent solution	—	—	—	1661	1679	—	—
Spray-dried from ethanol	1624	1638	1653	—	1673	1686	—
Crystalline	1624	—	1645	—	1672	1683	—
<i>Data from this study</i>							
Sample	$\beta$ -sheets*		$\gamma$ -loop	$\gamma$ -turn	Type-II $\beta$ -turn	MeBMT turn	Aggregate $\beta$ -sheet
Cosolvent solution	1630	—	—	1663	1678	—	—
10% wt/wt	1628	—	1653	—	1672	1684	—
20% wt/wt	1628	—	1653	—	1674	1684	—
30% wt/wt	1628	—	1653	—	1674	1684	—
50% wt/wt	1628	—	1653	—	1676	1686	—
Pure spray freeze-dried CsA	1626	1636	1653	—	1674	1688	—
Crystalline	1624	1636	1653	—	1674	1688	1695

\*In cyclosporine A, 2  $\beta$ -sheets occur: an antiparallel  $\beta$ -sheet (1624  $\text{cm}^{-1}$ ) and a looser  $\beta$ -sheet (1636  $\text{cm}^{-1}$ ).<sup>37</sup> In some samples both  $\beta$ -sheets overlap, resulting in a single  $\beta$ -sheet band at a wavenumber between 1624 and 1636  $\text{cm}^{-1}$ .

(—) indicates the particular structural element was not present in the sample as observed by FTIR measurements.

combination of a solid solution and suspension, ie, CsA is present in a molecular distribution and as clusters. Second, the presence of the  $\gamma$ -loop and corresponding cis orientation between MeLeu<sup>9</sup> and MeLeu<sup>10</sup> suggests an intramolecular orientation of D-Ala<sup>8</sup>NH, which suggests a lipophilic environment. Third, proximity of the MeBMT<sup>1</sup> side chain to the backbone suggests the presence of CsA clusters. Finally, the increasing intensity of the MeBMT-turn suggests that powders with higher drug loads contain more CsA clusters. Therefore, the amount of CsA in the form of solid suspension increases at higher drug loads.

The percentage of solid solution and solid suspension can be quantified by examination of the unresolved amide I bands. The amide I band depends on the orientation of the amide groups as shown in the secondary structure. The amide I band in the crystalline state clearly differs from the amide I in the cosolvent solution (Figure 4A). Furthermore, the amide I band of CsA in the inulin solid dispersion depends on the drug load (Figure 4B). As can be seen, the amide I band becomes more similar to the amide I band of the crystalline state with increasing drug loads.

By calculating the percentage of area-overlap of the different amide I bands relative to the amide I band of CsA in the cosolvent solution, it is possible to quantify the differences caused by an inter- to intramolecular change in rotation of the amide groups (Figure 5). CsA dissolved in the cosolvent solution mainly has an intermolecular orientation of the

amide groups as shown by analysis of the secondary derivative. In contrast, CsA in the crystalline state mainly has intramolecular orientation of the amide groups. Similar to the secondary structure, the percentage area overlap of the amide I band of both CsA in the solid dispersion and pure spray freeze-dried is in-between those of CsA in the cosolvent solution and crystalline CsA.

The 10% wt/wt solid dispersion already has 3.8% difference in percentage area overlap in comparison with CsA in the cosolvent solution, indicating that at a drug load of 10%, relatively much of the amide groups are oriented intramolecularly. The difference in percentage area overlap increases up to the 50% wt/wt solid dispersion. The 50% wt/wt solid dispersion has a difference in percentage area overlap, which is nearly the same as for pure spray freeze-dried CsA, indicating that the majority of the amide groups are intramolecularly orientated. Pure spray freeze-dried CsA has a difference in percentage area overlap of 8% with CsA in the cosolvent solution.

If on the one hand pure spray freeze-dried CsA is assumed to represent a complete solid suspension, and on the other hand CsA dissolved in the cosolvent solution to represent a complete solid solution, then it is possible to calculate the percentage of each type of solid dispersion. However, the polarity of the cosolvent solution and amorphous inulin presumably differs. As a result, the ability to establish orientation of the amide groups of CsA by the cosolvent solution in

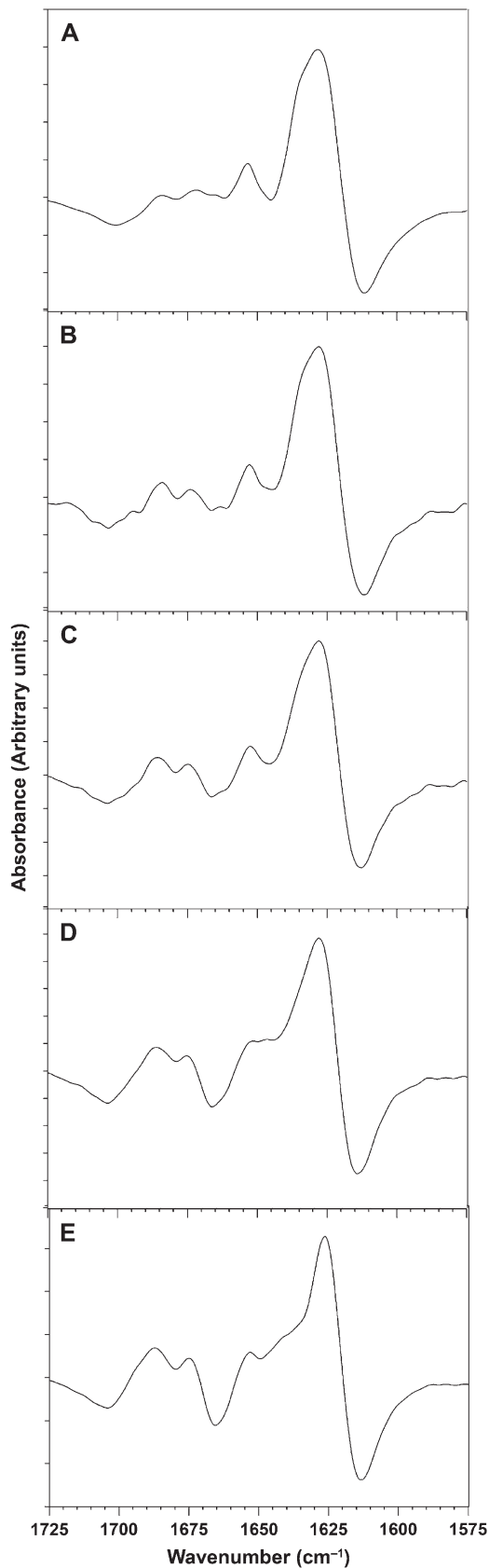


**Figure 3.** Second-derivative FTIR spectra of the 10% (A), 20% (B), 30% (C), and 50% (D) wt/wt solid dispersions and pure spray freeze-dried CsA (E). Peak wavenumbers: 1626 to 1628 ( $\beta$ -sheet), 1653 ( $\gamma$ -loop), 1672 to 1676 (type-II  $\beta$ -turn), and 1684 to 1688  $\text{cm}^{-1}$  (MeBMT-turn). See also Table 2.

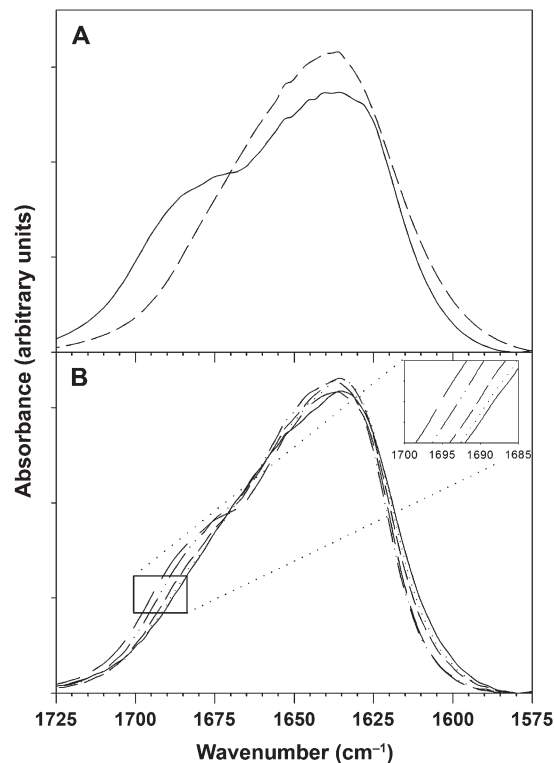


**Figure 4.** Baseline corrected and normalized amide I peak from FTIR spectra of CsA. (A) controls of crystalline CsA (—) and in MeOH/ACN/H<sub>2</sub>O (---). (B) Solid dispersions containing 10% wt/wt (—), 20% wt/wt (·····), 30% wt/wt (- · - · -), and 50% wt/wt (- - - -) CsA, and pure spray freeze-dried CsA (—).

comparison with inulin may therefore be different. The calculation thus only gives an indication about the percentage of type of solid dispersion. The 10% wt/wt solid dispersion has a 3.7% difference in percentage area overlap. When compared with the 8.1% difference in area overlap of pure

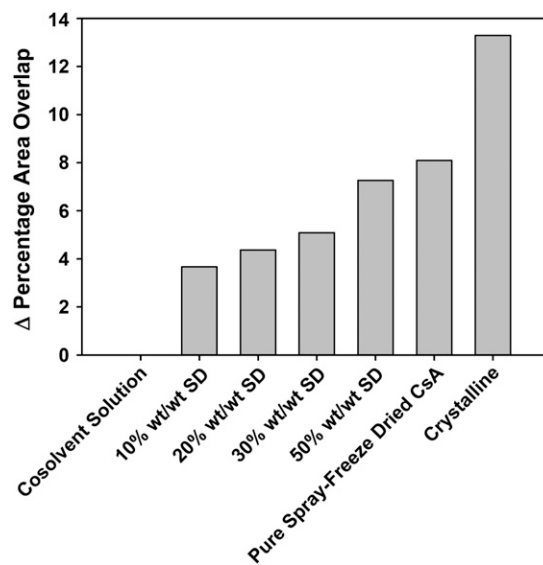


**Figure 5.** Difference in percentage area overlap of the amide I bands compared with the amide I band of CsA in the cosolvent solution.



spray freeze-dried CsA, which was assumed to represent a complete solid suspension, it follows that the 10% wt/wt solid dispersion contains 55% of CsA as a solid solution and 45% of a solid suspension. The 20%, 30%, and 50% wt/wt solid dispersion would then contain 54%, 63%, and 90% of the CsA as a solid suspension, respectively.

### Aerosol characteristics

Spray freeze-drying results in log-normal geometrical particle size distributions with relatively large volume median diameters ( $x_{50}$ ) (Table 3). The GSD of the spray freeze-dried solid dispersions, as calculated with Equation 1, are between 1.87 and 2.97 (Table 3).

To evaluate the aerodynamic behavior and measure the mass median aerodynamic diameter (MMAD), the powder was analyzed with cascade impactor analysis. As the powder showed rather cohesive behavior, a test inhaler, which is able to generate relatively high deagglomeration forces, was used.<sup>31</sup> Both the 30% and 50% solid dispersions exhibit excellent inhalation characteristics (Figure 6). The spray freeze-dried CsA solid dispersions show a low inhaler retention of approximately 4%, which leads to a high emitted fraction of approximately 96% for both solid dispersions (Figure 6). The solid dispersion powders furthermore show good dispersion characteristics as indicated by the respirable fraction of higher than 75%, as calculated by the sum of deposition on stages 2, 3, and 4 plus the filter. Furthermore, the FPF is higher than 50% of the metered dose, indicating that the solid dispersions are suitable for inhalation.

Since a volume median diameter ( $x_{50}$ ) is measured with laser diffraction and the particles were found to be spherical

**Table 3.** Particle Size Analysis:  $x_{16}$ ,  $x_{50}$ , and  $x_{84}$  Undersize Values of the Cumulative Geometric Size Distributions, MMAD, and GSD of the spray freeze-dried powders

Formulation	$x_{16}$ , $\mu\text{m}$	$x_{50}$ , $\mu\text{m}$	$x_{84}$ , $\mu\text{m}$	GSD, (-)	MMAD, $\mu\text{m}$
10% wt/wt CsA	3.08	7.10	17.10	2.36	—
20% wt/wt CsA	3.53	7.29	15.29	2.08	—
30% wt/wt CsA	3.52	6.84	12.32	1.87	3.50
50% wt/wt CsA	2.46	8.44	21.74	2.97	3.39
Pure spray freeze-dried CsA	2.94	8.81	19.43	2.57	—

MMAD indicates mass medial aerodynamic diameter; GSD, geometric standard deviation; CsA, cyclosporine A.

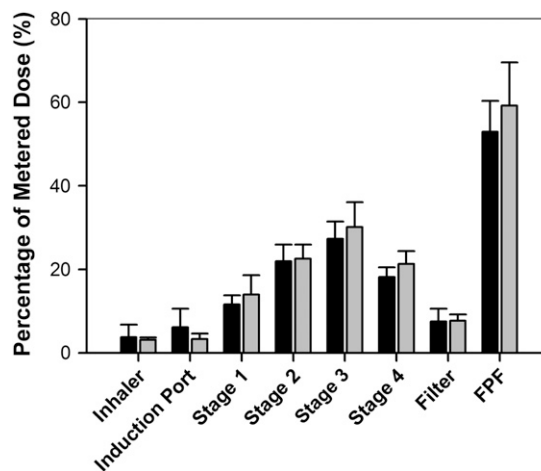


**Figure 6.** Cascade impactor analysis of the 30% (black bars) and 50% (gray bars) wt/wt solid dispersion at a flow rate of 60 L/min through an air classifier-based test inhaler. Error bars represent standard deviations ( $n = 3$ ).

(scanning electron microscopy, data not shown), we can assume that  $d_c$  equals  $x_{50}$  as obtained with laser diffraction. The MMAD can be measured by using the mean of the cut-off diameters (ie, 4.95 and 2.4  $\mu\text{m}$  for third and fourth stages, respectively, as calculated according to the European Pharmacopoeia<sup>39</sup>) and cumulative mass percentage.<sup>40</sup> The intercept at the 50% mass percentile of the cumulative mass percentage with cut-off diameter corresponds to the MMAD. Thus, we can rewrite Equation 2 to:

$$MMAD = x_{50} \sqrt{\rho_p} \quad (3)$$

In other words, by comparing the data obtained from laser diffraction and cascade impactor analysis, we can calculate the true particle density. The true particle density can be determined from the MMAD and volume median diameter if a log-normal distribution, a dynamic shape factor of 1, and a particle size independent density is assumed (Equation 3). The measured MMADs are 3.50 and 3.39  $\mu\text{m}$  for the 30% and 50% drug load solid dispersions, respectively (Table 3). Given Equation 3, it is possible to combine laser diffraction ( $x_{50} = d_c$ ) with cascade impaction data (MMAD) to calculate the density ( $\rho_p$ ) of the particles. The comparison results in a calculated density of 0.26 and 0.16  $\text{g}/\text{cm}^3$  for the 30% and 50% drug load solid dispersions, respectively. Since the true densities of CsA and inulin are around 1.5  $\text{g}/\text{cm}^3$ , the calculated density indicates the high porosity of the spray freeze-dried particles.

Spray freeze-drying of CsA and inulin resulted in relatively large ( $x_{50} \sim 7.5 \mu\text{m}$ ) but porous (low density) particles. In the literature,<sup>40-43</sup> several advantages are ascribed to the use of (large) porous particles for pulmonary administration such as high emitted dose (fraction that is released from the inhaler), good dispersion characteristics and high – deep – lung deposition. This was confirmed in this study.



## Dissolution

The dissolution rate of CsA formulated as a solid dispersion was significantly increased compared with the physical mixture, which consisted of pure spray freeze-dried CsA (Figure 7) and spray freeze-dried inulin. In the 10% and 20% wt/wt CsA-containing solid dispersions, inulin dissolves slightly faster than CsA (Figure 7A). The faster dissolution of inulin indicates that inulin dissolves first, followed by CsA. All solid dispersions dissolve faster than the physical mixture, albeit without a clear correlation between drug load and dissolution rate (Figure 7B). After 30 minutes, all solid dispersions have dissolved for more than 80% compared with only 50% of the physical mixture.

The improved dissolution rate of the solid dispersion powder can be ascribed to the presence of inulin in the solid dispersions for 2 reasons. First, the higher specific surface area of the solid dispersions, compared with pure spray freeze-dried CsA, will have contributed to the higher dissolution rate. Second, inulin improves wetting of CsA, even at drug loads up to 50%.

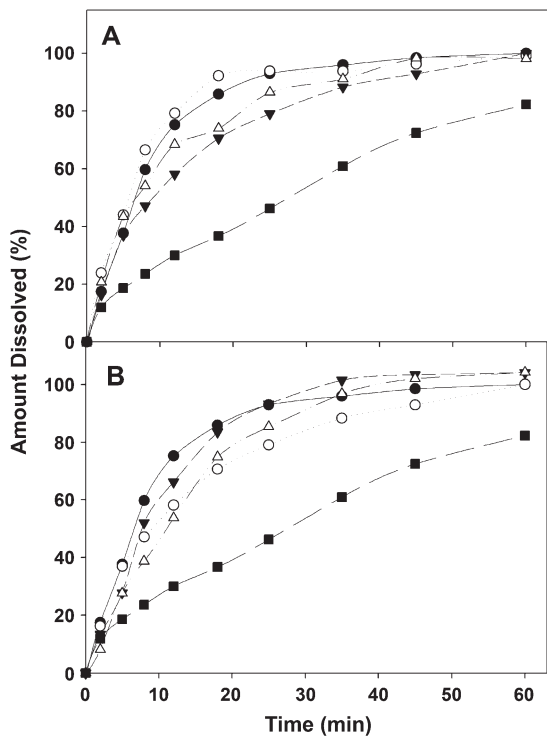


**Figure 7.** Dissolution behavior of the solid dispersions. (A) Dissolution behavior of a 10% (represented by circles) and 20% wt/wt (represented by triangles) solid dispersion. Open symbols represent inulin, closed symbols represent CsA. Squares represent the dissolution behavior of CsA from the physical mixture (30 mg CsA + 70 mg inulin). (B) Dissolution of CsA from the 10% (black circles), 20% (white circles), 30% (black triangles), and 50% (open triangles) solid dispersion and from the physical mixture (squares).

## CONCLUSION

In this study, a dry powder formulation containing CsA was developed for local administration in lung transplant patients. The presented dry powder formulations contain large porous particles that dissolve rapidly, even at high drug loads. The type of dry powder formulation was a solid dispersion. The solid dispersion, as investigated with FTIR, was found to be a mixture of a solid solution and a solid suspension, the ratio of which depended on the drug load. For inhalation, the high drug load formulations are especially favorable, since with these, a lower amount of powder has to be inhaled by the patient. Future studies will be performed to investigate whether this powder is a feasible alternative to nebulization and is able to improve therapeutic efficacy of treatment of lung transplant patients without increasing local and systemic side effects.

## REFERENCES

1. Corcoran TE, Smaldone GC, Dauber JH, et al. Preservation of post-transplant lung function with aerosol cyclosporin. *Eur Respir J.* 2004;23:378-383.
2. Iacono AT, Smaldone GC, Keenan RJ, et al. Dose-related reversal of acute lung rejection by aerosolized cyclosporine. *Am J Respir Crit Care Med.* 1997;155:1690-1698.
3. Iacono AT, Johnson BA, Grgurich WF, et al. A randomized trial of inhaled cyclosporine in lung-transplant recipients. *N Engl J Med.* 2006;354:141-150.
4. Burckart GJ, Smaldone GC, Eldon MA, et al. Lung deposition and pharmacokinetics of cyclosporine after aerosolization in lung transplant patients. *Pharm Res.* 2003;20:252-256.
5. Le Brun PPH, Vinks AA, Touw DJ, et al. Can tobramycin inhalation be improved with a jet nebulizer? *Ther Drug Monit.* 1999;21:618-624.
6. O'Callaghan C, Barry PW. The science of nebulised drug delivery. *Thorax.* 1997;52:S31-S44.
7. Touw DJ, Jacobs FA, Brimicombe RW, Heijerman HG, Bakker W, Briemer DD. Pharmacokinetics of aerosolized tobramycin in adult patients with cystic fibrosis. *Antimicrob Agents Chemother.* 1997;41:184-187.
8. Molpeceres J, Guzman M, Bustamante P, del Rosario Aberturas M. Exothermic-endothemic heat of solution shift of cyclosporin A related to poloxamer 188 behavior in aqueous solutions. *Int J Pharm.* 1996;130:75-81.
9. Van Drooge DJ, Hinrichs WLJ, Frijlink HW. Incorporation of lipophilic drugs in sugar glasses by lyophilization using a mixture of water and tertiary butyl alcohol as solvent. *J Pharm Sci.* 2004;93:713-725.
10. Le Brun PPH, de Boer AH, Mannes GP, et al. Dry powder inhalation of antibiotics in cystic fibrosis therapy: part 2. Inhalation of a novel colistin dry powder formulation: a feasibility study in healthy volunteers and patients. *Eur J Pharm Biopharm.* 2002;54:25-32.
11. Leuner C, Dressman J. Improving drug solubility for oral delivery using solid dispersions. *Eur J Pharm Biopharm.* 2000;50:47-60.
12. Sethia S, Squillante E. Solid dispersions: revival with greater possibilities and applications in oral drug delivery. *Crit Rev Ther Drug Carrier Syst.* 2003;20:215-247.

13. Kaushal AM, Gupta P, Bansal AK. Amorphous drug delivery systems: molecular aspects, design, and performance. *Crit Rev Ther Drug Carrier Syst.* 2004;21:133-193.
14. Van Drooge DJ, Hinrichs WLJ, Frijlink HW. Anomalous dissolution behaviour of tablets prepared from sugar glass-based solid dispersions. *J Control Release.* 2004;97:441-452.
15. Ericsson CH, Svartengren K, Svartengren M, et al. Repeatability of airway deposition and tracheobronchial clearance rate over three days in chronic bronchitis. *Eur Respir J.* 1995;8:1886-1893.
16. Moller W, Haussinger K, Winkler-Heil R, et al. Mucociliary and long-term particle clearance in the airways of healthy nonsmoker subjects. *J Appl Physiol.* 2004;97:2200-2206.
17. Johnson KA. Preparation of peptide and protein powders for inhalation. *Adv Drug Deliv Rev.* 1997;26:3-15.
18. Frijlink HW, De Boer AH. Dry powder inhalers for pulmonary drug delivery. *Expert Opin Drug Deliv.* 2004;1:67-86.
19. Maa YF, Nguyen PA, Sweeney T, Shire SJ, Hsu CC. Protein inhalation powders: spray drying vs spray freeze drying. *Pharm Res.* 1999;16:249-254.
20. van Drooge DJ, Hinrichs WL, Dickhoff BH, et al. Spray freeze drying to produce a stable Delta(9)-tetrahydrocannabinol containing inulin-based solid dispersion powder suitable for inhalation. *Eur J Pharm Sci.* 2005;26:231-240.
21. Zijlstra GS, Hinrichs WLJ, de Boer AH, Frijlink HW. The role of particle engineering in relation to formulation and de-agglomeration principle in the development of a dry powder formulation for inhalation of cetorelix. *Eur J Pharm Sci.* 2004;23:139-149.
22. van Drooge DJ, Hinrichs WL, Visser MR, Frijlink HW. Characterization of the molecular distribution of drugs in glassy solid dispersions at the nano-meter scale, using differential scanning calorimetry and gravimetric water vapour sorption techniques. *Int J Pharm.* 2006;310:220-229.
23. Salm P, Norris RL, Taylor PJ, Davis DE, Ravenscroft PJ. A reliable high-performance liquid chromatography assay for high-throughput routine cyclosporin A monitoring in whole blood. *Ther Drug Monit.* 1993;15:65-69.
24. Scott TA, Jr, Melvin EH. Determination of dextran with anthrone. *Anal Chem.* 1953;25:1656-1661.
25. Hinrichs WLJ, Prinsen MG, Frijlink HW. Inulin glasses for the stabilization of therapeutic proteins. *Int J Pharm.* 2001;215:163-174.
26. Dong A, Huang P, Caughey WS. Protein secondary structures in water from second-derivative amide I infrared spectra. *Biochemistry.* 1990;29:3303-3308.
27. Savitzky A, Golay MJE. Smoothing and differentiation of data by simplified least squares procedures. *Anal Chem.* 1964;36:1627-1639.
28. Kendrick BS, Dong A, Allison SD, Manning MC, Carpenter JF. Quantitation of the area of overlap between second-derivative amide I infrared spectra to determine the structural similarity of a protein in different states. *J Pharm Sci.* 1996;85:155-158.
29. van de Weert M, Haris PI, Hennink WE, Crommelin DJ. Fourier transform infrared spectrometric analysis of protein conformation: effect of sampling method and stress factors. *Anal Biochem.* 2001;297:160-169.
30. Ziegler J, Wachtel H. Comparison of cascade impaction and laser diffraction for particle size distribution measurements. *J Aerosol Med.* 2005;18:311-324.
31. de Boer AH, Hagedoorn P, Gjaltema D, Goede J, Frijlink HW. Air classifier technology (ACT) in dry powder inhalation: Part 1. Introduction of a novel force distribution concept (FDC) explaining the performance of a basic air classifier on adhesive mixtures. *Int J Pharm.* 2003;260:187-200.
32. Costantino HR, Firouzabadian L, Wu C, et al. Protein spray freeze drying. 2. Effect of formulation variables on particle size and stability. *J Pharm Sci.* 2002;91:388-395.
33. Rogers TL, Johnston KP, Williams RO, 3rd. Physical stability of micronized powders produced by spray-freezing into liquid (SFL) to enhance the dissolution of an insoluble drug. *Pharm Dev Technol.* 2003;8:187-197.
34. Molpeceres J, Aberturas MR, Guzman M. Biodegradable nanoparticles as a delivery system for cyclosporine: preparation and characterization. *J Microencapsul.* 2000;17:599-614.
35. Lee EJ, Lee SW, Choi HG, Kim CK. Bioavailability of cyclosporin A dispersed in sodium lauryl sulfate-dextrin based solid microspheres. *Int J Pharm.* 2001;218:125-131.
36. Liu C, Wu J, Shi B, Zhang Y, Gao T, Pei Y. Enhancing the bioavailability of cyclosporine a using solid dispersion containing polyoxyethylene (40) stearate. *Drug Dev Ind Pharm.* 2006;32:115-123.
37. Stevenson CL, Tan MM, Lechuga-Ballesteros D. Secondary structure of cyclosporine in a spray-dried liquid crystal by FTIR. *J Pharm Sci.* 2003;92:1832-1843.
38. Bertacche V, Pini E, Stradi R, Stratta F. Quantitative determination of amorphous cyclosporine in crystalline cyclosporine samples by Fourier transform infrared spectroscopy. *J Pharm Sci.* 2006;95:159-166.
39. European Pharmacopoeia(2.9.18) Procedure for powder inhalers Strasbourg: Council of Europe; 2005:249-250.
40. Vanbever R, Mintzes JD, Wang J, et al. Formulation and physical characterization of large porous particles for inhalation. *Pharm Res.* 1999;16:1735-1742.
41. Dunbar C, Scheuch G, Sommerer K, DeLong M, Verma A, Batycky R. In vitro and in vivo dose delivery characteristics of large porous particles for inhalation. *Int J Pharm.* 2002;245:179-189.
42. Edwards DA, Ben-Jebria A, Langer R. Recent advances in pulmonary drug delivery using large, porous inhaled particles. *J Appl Physiol.* 1998;85:379-385.
43. Edwards DA, Hanes J, Caponetti G, et al. Large porous particles for pulmonary drug delivery. *Science.* 1997;276:1868-1871.